Community structure follows simple assembly rules in microbial microcosms

Supplementary material

Figure S1. Competition experiments were performed by co-inoculating species and propagating them through five growth-dilution cycles. During each cycle, cells were cultured for 48 hours and then diluted by a factor of 1500 into fresh M9 media supplemented with Galacturonic acid and Serine as sole carbon sources. Community compositions were assessed by measuring the culture optical density (OD), as well as by plating on solid agar media and counting colonies, which are distinct for each species. Community composition was quantified at the end of the fifth cycle for all competitions, or at the end of every cycle in cases where the dynamics of competitions were investigated (**Fig. 2c**, **Fig. 3b**,**c**,**e**,**f**).

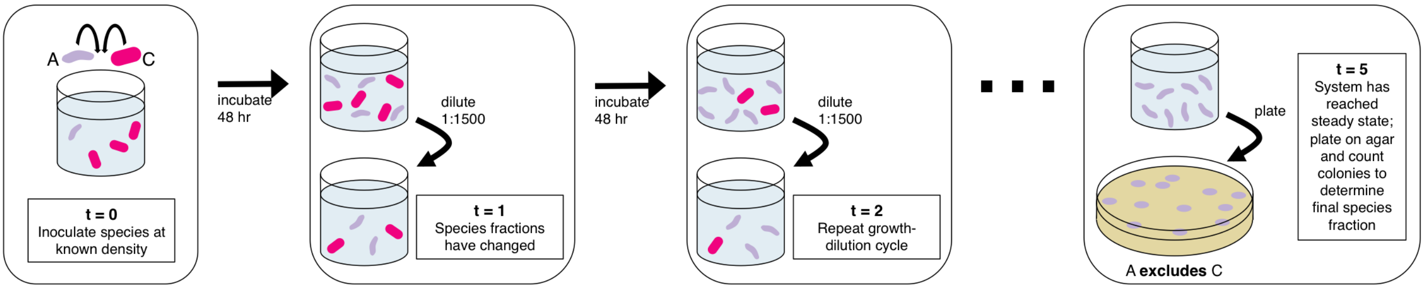

Figure S2. Growth rate in monoculture is correlated with competitive ability, but does not predict pairwise competitive outcomes. (a) Faster growing species tend to survive pairwise competitions more often than slow growers. (b) The probability that a fast-growing species will exclude a slow-growing species in pairwise competition increased with the difference between their growth rates. Nonetheless, even pairs which had a big discrepancy in growth rates where roughly as likely to coexist as they were to result in exclusion of the slow grower. To estimate growth rates, growth curves were measured for each species in a Tecan Infinite 200 Pro plate reader. Growth rates were estimated as the exponential growth rate which corresponds to the measured time it took each species to reach a given optical density (10^{-2}) from a known initial density ($\sim 10^{-4}$). These growth rates account for any initial lag time, or slower growth period, which may impact species' competitive performance.

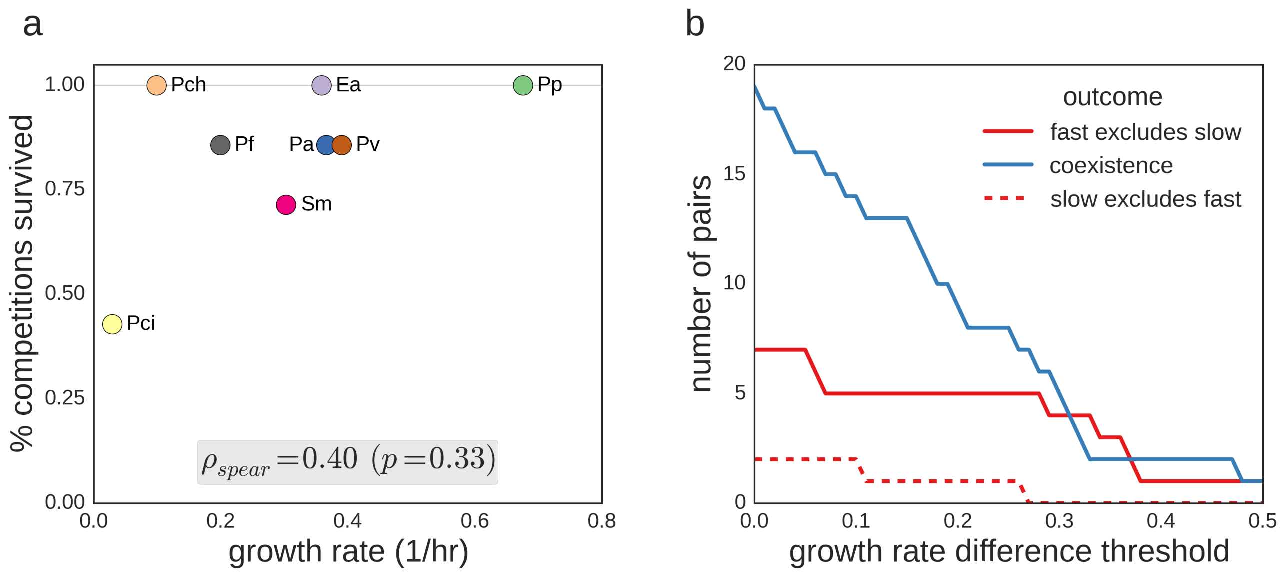

Figure S3. Inconsistent trio outcomes are likely due to rapid evolution. (a,b) In two trios we observed high variability in competitive outcomes between initial conditions, as well as between replicates. Both of these cases involved a common pair of species: Ea-Pv. The triangle are simplex plots, with edges indicating the pairwise outcomes, and dots denoting the fractions of species at the end of competitions. Dot colors indicate the initial condition of the competition: at the beginning of competition, the species with the corresponding color was present at 90% of the total cell density, and the other two species were at 5% each. Competitions starting from each initial condition were done in duplicate. (c) To test whether this variability could arise during the experiment, we performed additional competitions between Ea and Pv, involving eight biological replicates and six initial fractions for each replicate. For each biological replicate, a colony of each species was picked at the beginning of the experiment and grown in rich media and subsequently in the experimental media prior to the beginning of competitions (**Methods**). While all competitions resulted in the coexistence of both species, the coexistence fraction varied significantly. Most of this variability occurred across the biological replicates, potentially indicating adaptation during the growth prior to the beginning of competitions. (d) Fraction trajectories for two initial conditions of three of the biological replicates, highlighting the variability between biological replicates.

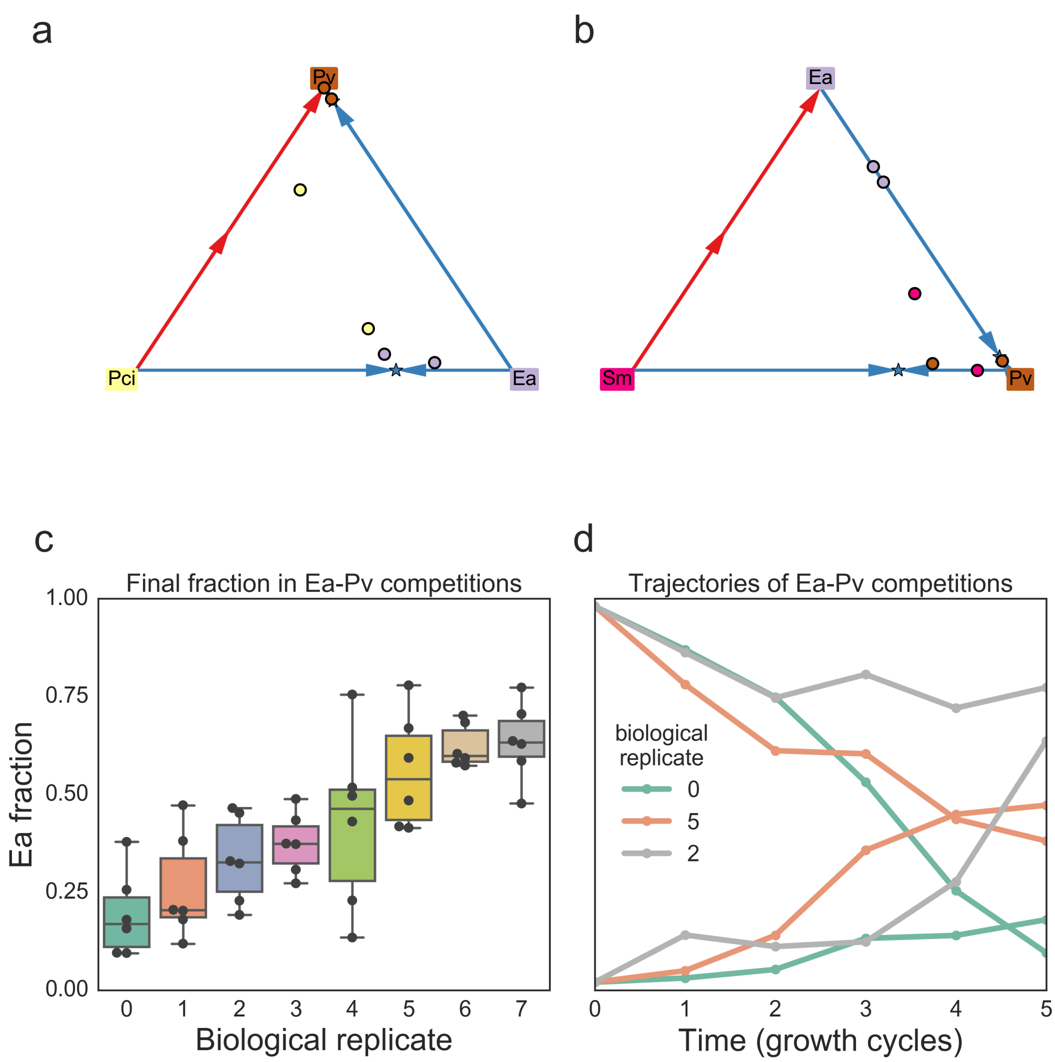

Figure S4. Inter-species interactions included interference competition and facilitation (a) Several species grew to a higher density in the presence of an additional species than in monoculture. The impact of each competitor on each focal species was quantified by calculating its relative yield, defined as: (density in coculture - density in monoculture)/(density in coculture + density in monoculture). A negative relative yield indicates growth hindrance, whereas positive values indicated facilitation. (b) Interference competition was detected by growing species on supernatant media in all pairwise combinations. Supernatant was obtained by filter sterilizing experimental media in which monocultures were grown for 48hr. The supernatant media was composed of supernatant supplemented with carbon sources and nutrients to minimize the effect of resource depletion. Species were grown in the supernatant media, and their final density when grown of supernatant obtained from other species was compared to the density achieved when grown on their own supernatant by calculating a relative yield defined as: (density on other supernatant - density on self supernatant)/(density on other supernatant + density on self supernatant).

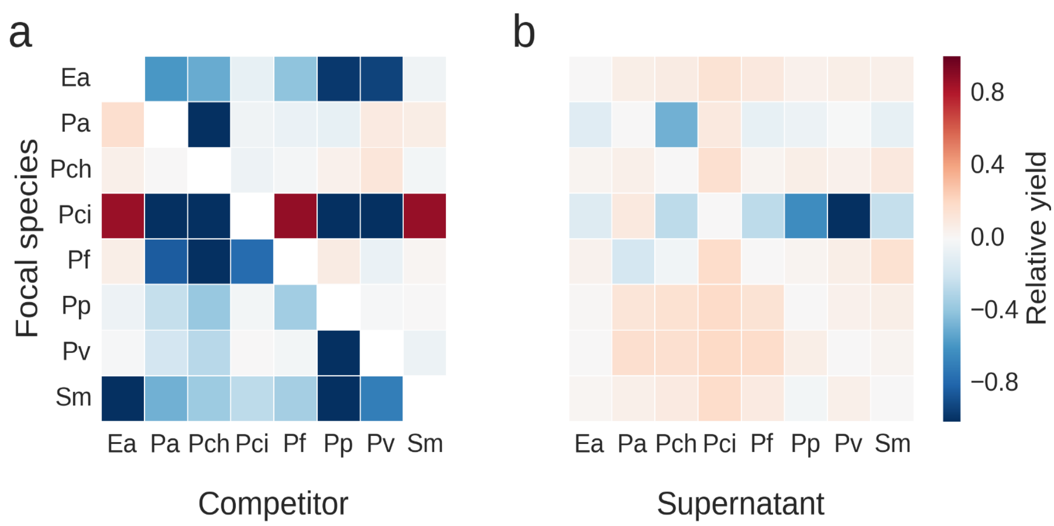

Figure S5. The gLV model, fitted to experimental data, does not improve predictability over the assembly rule. gLV model parameters were inferred from time trajectories of monocultures and pairwise competitions (**Fig. S7**). The inferred parameter values were used to simulate trio competitions (a) or competitions between sets of seven and eight species (b), and predict species survival.

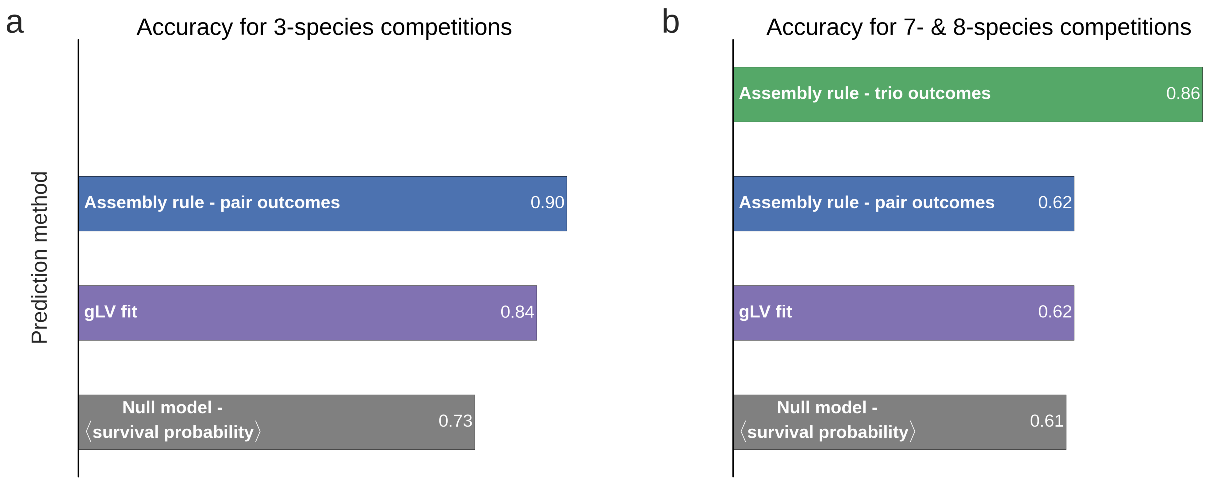

Figure S6. gLV simulations recapitulate the experimentally observed proportions of pair outcomes, and yield a distribution of trio layouts similar to the observed one. (a) gLV simulations included only pairs displaying competitive exclusion or coexistence, in proportions tmatching the experimentally observed ones. Bistable pairs that were generated in the simulation were discarded. (b) The majority of trio layouts that occurred in the simulations were also observed experimentally, with a median of ~4/56 novel trio layouts occurring in the simulations. Medians and interquartile ranges (IQR) of occurrences in simulations are computed using 100 independent simulations. For each simulation, we created a set of eight species with random interactions strengths (α_{ij}) independently drawn from normal distribution with a mean of 0.6 and a standard deviation of 0.46. Pairwise outcomes and trio layouts were determined from the interaction strengths.

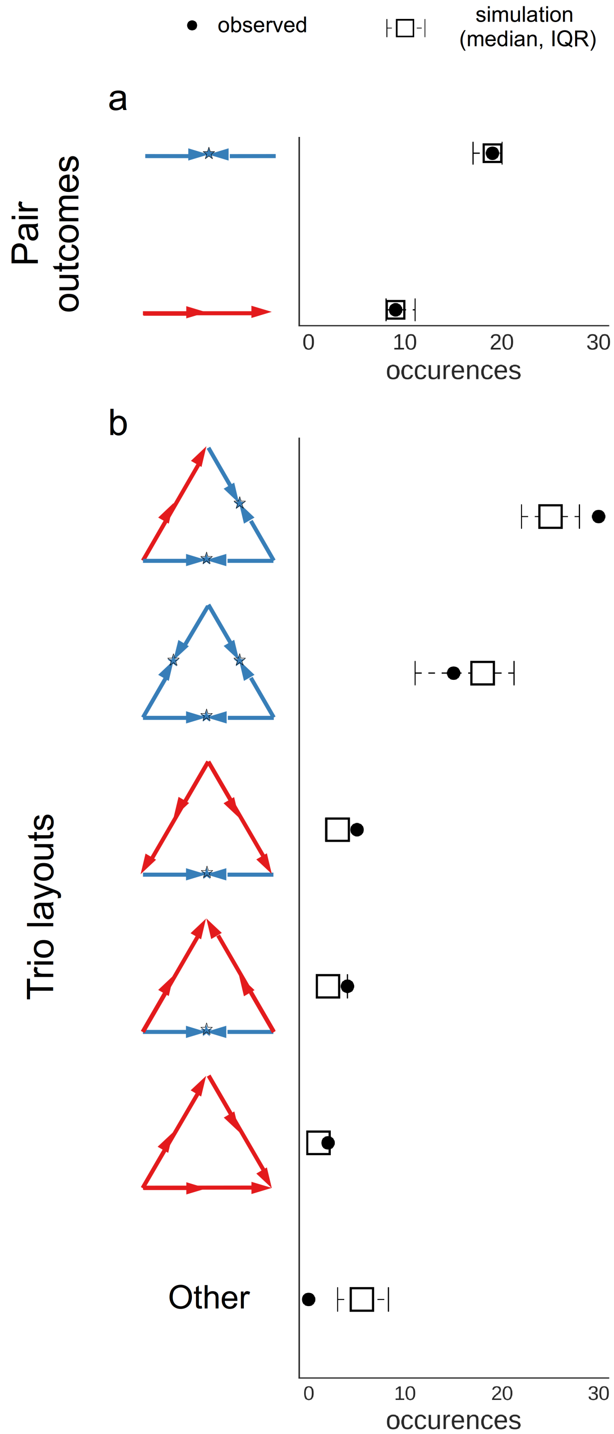

Figure S7. gLV model parameters were fitted to the trajectories of monocultures and pair competitions. (a) A growth rates (r) and carrying capacity (K) was fitted to each monoculture trajectories, using eight replicates per species (**Table S2**). (b) Interaction coefficients (α_{ij}) where fitted to trajectories of pair competitions, using the inferred growth rates and carrying capacities (**Table S3**). Each pair was competed in duplicate from two initial conditions where one species constituted 95% of the community and the other 5%. Some data are missing due to contamination or failed plating. Each species' OD was determined from the total culture OD and the species fractions, as measured by colony counting. Fits were done by simulating the growth and dilution cycles with gLV dynamics within a cycle, and minimizing the root-mean-square difference between the simulated dynamics and observed ones. The minimization was done using the Nelder-Mead method, as implemented in the *minimize* function from the python scipy package (v 0.16.0).

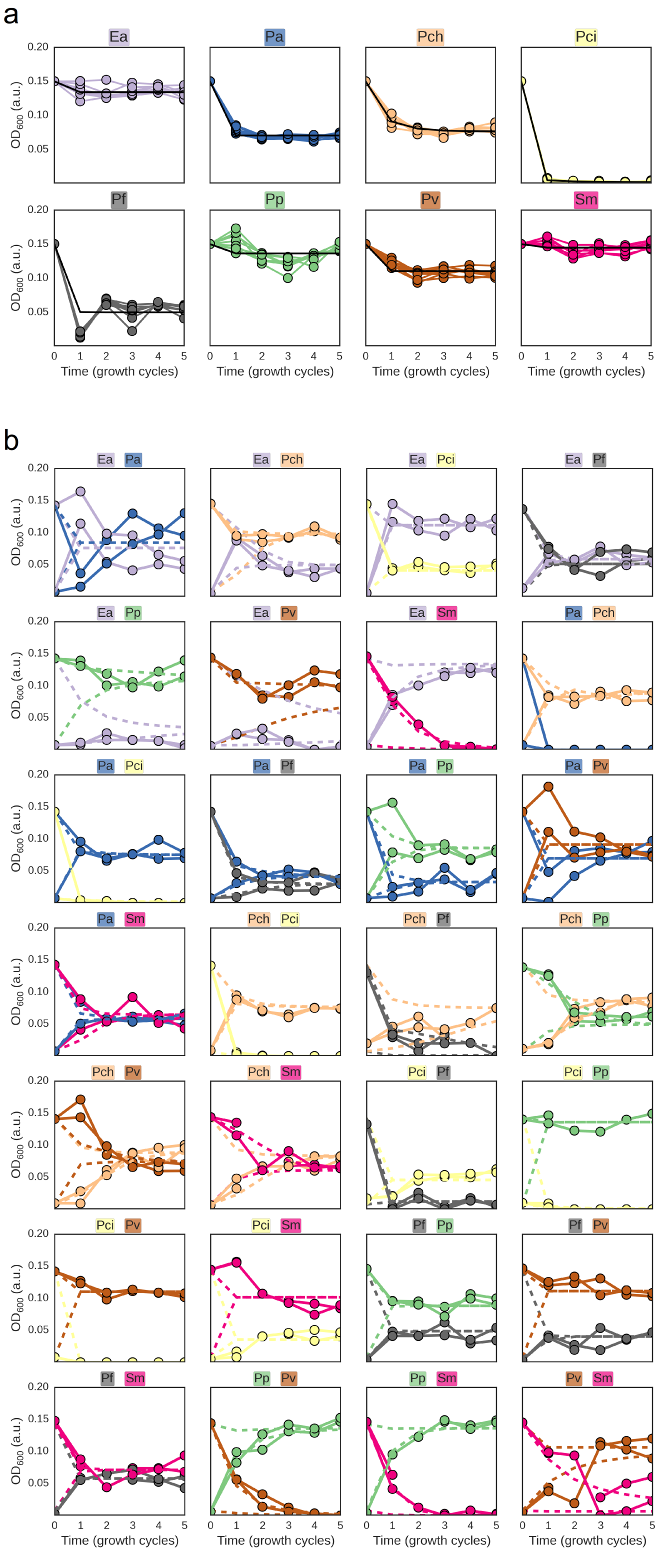

Table S1. Trio competitions typically resulted in a stable community whose composition is independent of the starting fractions. Only a single trio (Pp, Pch, Sm) showed consistent bistability, with species survival depending on the initial community composition. Trios are sorted by layout and competitive outcomes. Species are ordered to match the layouts shown in **Fig 3**. Survival (extinction) is indicated by a value of 1 (0). Survival values are not indicated for the two trios that did not display reproducible outcomes (**Fig. S3**).

Competitors			**Survival**		
species A	species B	species C	species A	species B	species C
Ea	Pa	Sm	1	1	0
Ea	Pch	Pa	1	1	0
Ea	Pch	Sm	1	1	0
Ea	Pf	Sm	1	1	0
Pa	Ea	Pci	1	1	0
Pa	Pf	Pci	1	1	0
Pa	Sm	Pci	1	1	0
Pch	Ea	Pci	1	1	0
Pch	Ea	Pf	1	1	0
Pch	Pp	Pf	1	1	0
Pch	Sm	Pci	1	1	0
Pp	Ea	Pv	1	1	0
Pp	Pa	Pv	1	1	0
Pp	Pa	Sm	1	1	0
Pp	Pch	Pa	1	1	0
Pp	Pf	Pci	1	1	0
Pp	Pf	Pv	1	1	0
Pp	Pf	Sm	1	1	0
Pv	Pch	Pa	1	1	0
Pv	Pf	Pci	1	1	0
Pv	Sm	Pci	1	1	0
Sm	Pch	Pa	1	1	0
Ea	Pci	Sm	1	1	1
Pch	Pv	Pf	1	1	1
Pch	Sm	Pf	1	1	1
Pp	Ea	Pci	1	1	1
Pp	Pch	Pv	0	1	1
Pp	Pch	Sm	1	1	0
			0	1	1

Ea	Pv	Sm	na	na	na
Pv	Ea	Pci	na	na	na
Pf	Pa	Sm	1	1	1
Pf	Pci	Ea	1	1	1
Pf	Pp	Ea	1	1	1
Pf	Pv	Ea	1	1	1
Pf	Sm	Pci	1	1	1
Pp	Pa	Ea	1	1	1
Pv	Pa	Ea	1	1	1
Pv	Pch	Ea	1	1	1
Pf	Pa	Ea	0	1	1
Pf	Pa	Pp	0	1	1
Pf	Pa	Pv	0	1	1
Pf	Sm	Pv	0	1	1
Pp	Pch	Ea	0	1	1
Sm	Pa	Pv	0	1	1
Sm	Pv	Pch	0	1	1
Pci	Pp	Pa	0	1	1
Pci	Pp	Pch	0	1	1
Pci	Pv	Pa	0	1	1
Pci	Pv	Pch	0	1	1
Sm	Pp	Ea	0	1	1
Pch	Pf	Pci	1	0	0
Pf	Pch	Pa	1	0	0
Pp	Sm	Pci	1	0	0
Pp	Sm	Pv	1	1	1
Pci	Pch	Pa	0	1	0
Pv	Pp	Pci	0	1	0

Table S2. Inferred growth rates and carrying capacities.

	r	k
Ea	0.46	0.13
Pa	0.55	0.07
Pch	0.18	0.11
Pci	0.16	0.01
Pf	0.25	0.05
Pp	0.65	0.14
Pv	0.57	0.11
Sm	0.34	0.15

Table S3. Inferred interspecies interaction parameters. Note that these are interaction parameters (a_{ij}) which are not normalized by the carrying capacity. The corresponding gLV equations are:

$$\dot{N}_i = r_i N_i \left(1 - \frac{\sum_j a_{ij} N_j}{K_i}\right).$$

	Ea	**Pa**	**Pch**	**Pci**	**Pf**	**Pp**	**Pv**	**Sm**
Ea	1	0.69	1.09	0.55	1.53	0.82	1.09	0.72
Pa	-0.18	1	2.44	-2.58	1.13	0.43	0.01	0.21
Pch	-0.11	-0.8	1	-15.75	0.29	-0.04	-0.05	-0.03
Pci	-0.32	0	0.18	1	-3.39	0	0.05	-0.3
Pf	-0.02	0.28	1.2	0.83	1	0.01	0.07	-0.1
Pp	0.87	1.58	1.24	0.24	1	1	1.01	0.84
Pv	0.83	0.28	0.47	0	-0.02	0.79	1	0.7
Sm	0.96	1.23	1.42	1.21	1.31	0.91	0.98	1